Intramolecular Interactions in Chemically Modified *Escherichia coli* Thioredoxin Monitored by Hydrogen/Deuterium Exchange and Electrospray Ionization Mass Spectrometry†

Moo-Young Kim,‡ Claudia S. Maier,‡ Donald J. Reed,§ P. Shing Ho,*,§ and Max L. Deinzer*,‡

Department of Chemistry and Department of Biochemistry and Biophysics, Oregon State University, Corvallis, Oregon 97331

Received August 1, 2001; Revised Manuscript Received September 28, 2001

ABSTRACT: Site specific amide hydrogen/deuterium content of oxidized and reduced *Escherichia coli* thioredoxin, and alkylated derivatives, Cys-32-ethylglutathionylated and Cys-32-ethylcysteinylated thioredoxins are measured, after exposure for 20 s to D_2O/phosphate buffer (pH 5.7), by electrospray mass spectrometry. The degree of deuteration of Oxi-TRX and Red-TRX correlated with the rates of H/D exchange measured previously by NMR. The ethylcysteinyl modification was shown to minimally perturb the active site of the reduced protein, but showed more global effects on structures of α-helices and β-strands distant from the site of modification. In contrast, the larger ethylglutathionyl group had little effect on the protein's overall conformation, but significantly affected the structure of loops close to the active site. A molecular model of GS-ethyl-TRX derived from molecular simulation allowed the H/D exchange results to be interpreted in terms of specific interactions between the alkyl chain and the protein surface. The specific conformation of the ethylglutathione modification was predicted to be fixed by salt bridges between the carboxylates of the γ-Glu and Gly of glutathione and the guanidinium of Arg-73 and ϵ-amino group of Lys-90 of the protein. Specific hydrogen bonding interactions between the glutathione carbonyl oxygens and the amide protons of thioredoxin residues Ile-75 and Ala-93 were predicted. The H/D exchange studies showed low levels of deuterium incorporation at backbone nitrogens of these residues. The data also provided evidence for an unusual amide proton−amide nitrogen hydrogen bond within the ethylglutathionylated chain. These same sets of electrostatic and hydrogen bonding interactions were not predicted or observed for the smaller alkyl modification in Cys-ethyl-TRX.

Chemical modification of a protein can perturb the conformation, the folding and unfolding profile, and its stability in the presence of denaturing agents or at pH and temperature extremes (*1*, *2*). Such changes in the structure of proteins can be monitored by multidimensional nuclear magnetic resonance (NMR),[1] while changes in dynamics are reflected in the rates of hydrogen/deuterium (H/D) exchange (*3*−*10*) as measured by NMR or mass spectrometry. The goal of this study is to use H/D exchange and mass spectrometry to assess the extent of structural changes in *Escherichia coli* thioredoxin (TRX) modified by the episulfonium ion derived from *S*-(2-chloroethyl)glutathione (CEG) and *S*-(2-chloroethyl)cysteine (CEC).

TRX has been well-characterized biochemically and structurally; the high-resolution structures of oxidized and reduced forms of *E. coli* TRX have been determined by X-ray crystallography (*11*) and NMR spectroscopy (*12*−*14*). The disulfide linkage between Cys-32 and Cys-35 at the active site of Oxi-TRX can be reduced by the flavoprotein enzyme thioredoxin reductase through its NADPH cofactor (*15*). Alkylation or site-directed mutagenesis of either cysteine residue causes a loss of activity of TRX. Aside from the obvious effects on the ability to oxidize the active site residues, there remains a question as to whether such modifications will significantly affect the conformation of TRX. For example, the ^{1}H NMR spectra of a C35A mutant of *E. coli* thioredoxin are nearly identical to that of the wild-type protein, demonstrating the overall similarity in their structures (*16*). The resonances of some amide protons are shifted in the mutant, but the most significant perturbations were observed in the resonances of I75 and P76, residues which are within van der Waals contact of the mutated site. In addition, a 16-amino acid peptide covalently attached to Cys-32 of the C35A mutant shifts the pK_a of Asp-26 from 7.4 to 9.2 by shielding the region from solvent. Otherwise, the modification appears to have little additional structural effect on reduced thioredoxin that had not already been seen in the C35A mutant.

In contrast, the mutation of four cysteines to serines in human thioltransferase (TTase) containing only the active

† This work was supported by the NIH (NIEHS Grants ES00040 and ES00210) and by the NSF (Grant MCB-0090615 to P.S.H.).

* To whom correspondence should be addressed. Telephone: (541) 737-1773. Fax: (541) 737-0497. E-mail: max.deinzer@orst.edu (M.L.D.) or hops@ucs.orst.edu (P.S.H.).

‡ Department of Chemistry.

§ Department of Biochemistry and Biophysics.

[1] Abbreviations: AMBER, assisted model building with energy refinement; CEC, *S*-(2-chloroethyl)cysteine; CEG, *S*-(2-chloroethyl)-glutathione; CID, collision-induced dissociation; H/D, hydrogen/deuterium; HPLC, high-performance liquid chromatography; MS, mass spectrometry; MS/MS, tandem mass spectrometry; NADPH, nicotinamide adenine dinucleotide phosphate (reduced); NMR, nuclear magnetic resonance; PDB, Protein Data Bank; TCEP, tris(2-carboxyethyl)phosphine; TRX, *E. coli* thioredoxin (Oxi, oxidized; Red, reduced; GS-ethyl, Cys-32-ethylglutathionylated; Cys-ethyl, Cys-32-ethylcysteinylated); TTase, human thioltransferase.

10.1021/bi0115941 CCC: $20.00
Published on Web 11/06/2001

site Cys-22 residue with covalently attached glutathionyl group to form the mixed disulfide intermediate (TTase-SSG) shows similar specificity but greatly enhanced catalytic efficiency toward other glutathionyl mixed disulfide substrates (*17*). Apparently, the overall structure of the protein and not the chemical properties of the cysteine residues is important to the regulation of this particular biological activity, and the adduction by groups through the mixed Cys-22 disulfide appears to improve the stability to the protein's tertiary structure.

In the studies presented here, the levels of H/D exchange in the structures of Oxi-TRX and Red-TRX were determined by mass spectrometry. These results are correlated to residues that have been previously defined as structured and nonstructured from prior NMR studies (*13*) to determine the degree to which mass spectrometry can be used to probe protein tertiary structure at the level of individual amino acids. In addition, the structures of the alkylation products at Cys-32 of TRX [Cys-32-ethylglutathionylthioredoxin (GS-ethyl-TRX) and Cys-32-ethylcysteinylthioredoxin (Cys-ethyl-TRX)] were studied by mass spectrometry to determine the effect of such modifications on the conformation of the protein. Vicinal dihaloethanes are manufactured in large quantities, and because of their volatility, they become major environmental problems. It is well-known that these chemicals have significant toxicological effects that are in part mediated by alkylation of glutathione which in turn alkylates thioredoxin, other proteins, and nucleic acids via the episulfonium ion (*18*−*20*). It can be hypothesized that the active sites of proteins containing a "thioredoxin fold", i.e., Cys-X-X-Cys, such as thioredoxin, thioredoxin reductase, and protein disulfide isomerase are in vivo targets for alkylation by glutathione conjugates. The mass spectrometry results for the ethylglutathionyl variant are interpreted at the atomic level in the context of a molecular model constructed for the GS-ethyl-TRX protein.

MATERIALS AND METHODS

Alkylation of TRX. The disulfide linkage of *E. coli* thioredoxin (Promega, 200 μg, 0.02 μmol) was reduced by addition of 17 μL of 8 mM tris(2-carboxyethyl)phosphine hydrochloride (TCEP-HCl, Pierce) and incubated for 10 min to yield a 1.2 mM solution of Red-TRX. The reduction reaction was monitored by reverse-phase HPLC. Aliquots of Red-TRX (17 μL) were mixed with equal volumes of 0.4 M ammonium bicarbonate buffer (pH 7.7). The alkylating agents, *S*-(2-chloroethyl)glutathione (CEG) and *S*-(2-chloroethyl)cysteine (CEC), were prepared as described previously (*19*). CEG (184 μg, 0.5 μmol, 25 equiv) was dissolved in 33 μL of 0.4 M ammonium bicarbonate buffer (pH 7.7) and quickly added to the Red-TRX solution. The pH dropped slightly with the addition of CEG so that the pH of the reaction mixture was between 7.0 and 7.4. The reaction was monitored by reverse-phase HPLC. The reaction mixtures were incubated for 90 min at room temperature. More CEG (2×265 μg) was added until the Red-TRX was completely consumed. {*S*-[2-(Cys^{32})Ethyl]glutathione}thioredoxin (GS-ethyl-TRX) was isolated by semipreparative reverse-phase HPLC on a C4 column (250 mm $\times$ 10 mm, 5 μm, Vydac). The elution gradient was linear from 20 to 40% B over the course of 10 min, then to 50% B over the course of 15 min, and finally to 70% B over the course of 10 min; the flow rate was 2.5 mL/min. Solvent A was 0.1% TFA/H_2O, and solvent B was 0.1% TFA/CH_3CN. After the collected eluent had been freeze-dried, 144 μg (70%) of GS-ethyl-TRX was obtained. {*S*-[2-(Cys^{32})Ethyl]cysteine}thioredoxin (Cys-ethyl-TRX) was prepared from CEC by the same procedure. After HPLC purification and drying, 160 μg (80%) of Cys-ethyl-TRX was obtained.

Deuterium Exchange, Peptic Digestion, Mass Spectrometry, and HPLC (21). Oxidized *E. coli* thioredoxin was purchased from Promega (Madison, WI). Red-TRX was obtained by dissolving Oxi-TRX (0.85 mM) in 8 mM TCEP/phosphate buffer (10 mM, pH 5.7). Modified TRXs (GS-ethyl-TRX and Cys-ethyl-TRX) were equilibrated at 45 °C in phosphate buffer (10 mM, pH 5.7) for 20 min to establish a stabilized conformer and cooled to room temperature. The concentration of TRX (Oxi-, Red-, GS-ethyl-, and Cys-ethyl-TRX) stock solutions is 0.85 mM in phosphate buffer (H_2O, 10 mM, pH 5.7, 25 °C). TRXs were labeled by diluting the solution 20-fold with D_2O (phosphate, pD 5.7, 25 °C). Solutions were maintained at room temperature (25 °C), and isotope exchange was allowed for 20 s. Aliquots (5 μL, 200 pmol) of a diluted solution were adjusted to pH 2.5 by the addition of 0.1 M HCl and cooled to 0 °C. Immediately after quenching had been carried out, exchanged TRX aliquots were digested at 0 °C by adding 1 μL of a precooled pepsin solution (3 mg/mL in 5% formic acid) for 5 min. Aliquots (5 μL) were taken from the digest and loaded onto a microbore HPLC column (20 cm $\times$ 0.32 mm, 15 μm, LUNA C18) in an ice bath. The peptic peptides were separated over a 10 min period with a 25 to 70% acetonitrile/water gradient containing 0.05% trifluoroacetic acid. The column effluent (30 μL/min) was delivered directly to a Finnigan LCQ ion-trap mass spectrometer for ESI-MS and ESI-MS/MS experiments. Xcalibur and MagTran software in an IBM personal computer were used for instrument control, data acquisition, and data processing.

Molecular Model for GS-Ethyl-TRX. To construct a model for the ethylglutathionyl-modified protein, we started with the 2.2 Å resolution single-crystal structure of oxidized thioredoxin from *E. coli* (PDB code 1TXX) (*22*). All model building and reconstructions were performed using the InsightII molecular modeling program (Biosym/MSI, San Diego, CA), and subsequent molecular mechanical simulations were performed using the AMBER force field (*23*, *24*) as implemented in the Discover module of InsightII. The disulfide bond between the β-sulfurs of Cys-A32 and Cys-A35 was broken, and hydrogens were added to both Cys residues. The entire protein structure was subjected to energy minimization to relieve strain in the starting model. The glutathionyl group was constructed with the amino acids in their extended conformations off the sulfur of Cys-32 using the Biopolymer module of the InsightII program. With the atoms of the protein fixed, the glutathionyl chain was subjected to a systematic set of rigid rotations about the four bonds of the ethyl link between Cys-32 and the Cys residue of the glutathionyl modification. This search resulted in four classes of rotamer conformations with no major collisions near the site of attachment. The glutathionyl chain in each of these four rotamers was then subjected to a series of molecular dynamics simulations and energy minimizations, again with the atoms of the protein fixed, to adapt each rotamer of the glutathionyl chain to the protein structure.

Table 1: Deuterium Levels Found at Individual Amide Linkages in Fragments of Residues 59−79 (GS-Ethyl- and Cys-Ethyl-TRX) and 59−80 (Oxi- and Red-TRX) of 20 s Labeled TRXs

	no. of Ds on residue[a]				log k_{ex} (s^{-1})[b]			
residue	Oxi-TRX	Red-TRX	GS-ethyl-TRX	Cys-ethyl-TRX	Oxi-TRX		Red-TRX	
Gln-62	−	−	0.1	−	−2.72	S	−3.1	S
Asn-63	−	0.1	0.5	0.1	−4.8	S	−4.62	S
Pro-64	−	−	−	−				
Gly-65	0.6	0.9	0.7	0.9	*b*	M	*b*	M
Thr-66	0.2	0.2	0.1	0.8	−4.36	S	−4.15	S
Ala-67	−0.1	0.2	0.2	0.7	−4.66	S	−4.54	S
Pro-68	−	−	−	−				
Lys-69	0.1	0.1	0.3	0.3	−3.21	S	−3.09	S
Tyr-70	0.0	−0.1	0.3	0.2	−5.06	S	−4.91	S
Gly-71	(0.3)	(0.4)	(0.9)	(0.9)	*b*	M	−0.31	F
Ile-72	(0.3)	(0.4)	(0.9)	(0.9)	−3.69	S	−3.52	S
Arg-73	0.7	0.7	1.0	1.0	−0.14	F	−0.2	F
Gly-74	(0.9)	0.8	1.0	1.0	−0.19	F	0.23	F
Ile-75	(0.9)	0.8	0.1	0.9	*b*	M	−0.01	F
Pro-76	−	−	−	−				
Thr-77	0.2	0.3	0.2	0.1	−4.37	S	−3.82	S
Leu-78	0.2	0.3	0.1	0.2	−5.74	S	−5.67	S
Leu-79	0	0.3	0.2	0.1	−7.6	S	−7.6	S
Leu-80	0.1	0.2	−	−	−8	S	−8	S

[a] In cases of missing fragment ions, the difference of deuterium numbers was equally divided into possible sites as shown in parentheses. [b] The intermediate exchange rates are designated as M, which is in the range of 0.0025−0.25 s^{-1} (log value of −2.6 to −0.6).

Finally, the overall structures of the glutathionyl-modified proteins were subjected to molecular dynamics at low temperatures (300 K) and energy minimized. The structure having the lowest overall potential energy was defined as the ethylglutathionylthioredoxin (GS-ethyl-TRX) model.

RESULTS

The conformations of TRX in its oxidized (Oxi-TRX) and reduced (Red-TRX) states and the alkyl-modified GS-ethyl-TRX and Cys-ethyl-TRX protein forms were probed by following the rates of H/D exchange of the amide protons located along the polypeptide backbone. These rates were measured at the residue level by collision-induced dissociation tandem mass spectrometry (CID MS/MS), explicitly monitoring the b_n ions. For the overall protein, the method correlates well with NMR results for TRX in its oxidized and reduced states, and distinguishes between conformationally flexible and nonflexible regions of the protein at the residue level. For the GS-ethyl- and Cys-ethyl-modified TRX proteins, additional changes are evident in the exchange rates in terms of how the alkyl modifications affect the surface of the TRX protein in a molecular model.

Residue Specific Hydrogen Isotope Exchange of Oxidized and Reduced TRX. H/D exchange rates at individual amide linkages of TRX were determined by CID MS/MS after incubating the oxidized and reduced forms of the protein in D_2O (phosphate buffer, 10 mM, pH 5.7) for 20 s. To correlate the rates measured here by mass spectrometry with those determined previously by spectroscopy (*13*), the hydrogens for Oxi-TRX and Red-TRX were classified according to their NMR rates of H/D exchange (Tables 1−3). Hydrogens seen by NMR to undergo fast exchange (with exchange rates log $k_{ex} > -0.6$ s^{-1}) are designated as F and those exchanging slowly (log $k_{ex} < -2.6$ s^{-1}) designated S. These encompass the ranges that can be obtained by the NMR methods. Amide protons whose exchange rates are too slow to measure by saturation transfer but exchange too fast to be observed by NMR fall in the range -2.6 $s^{-1} <$ log $k_{ex} < -0.6$ s^{-1} and are designated as M for having medium rates of exchange. As expected, the amide protons involved in hydrogen bonds within well-defined secondary structures (e.g., in α-helices) and buried from the surface (as in the β4 strand of the β-sheet) show slow exchange, while those at less structured loops and exposed regions are in the faster exchange group (Figure 1). The hydrogens of Cys-35 at the active site and the associated amino acids in the loop, not surprisingly, become overall more readily exchangeable upon reduction of the disulfide bond to Cys-32 (Figure 1B,C).

Deuterium levels determined here by mass spectrometry at amide sites generally correlate well with the exchange rate constants for the b_n ions for Oxi-TRX and Red-TRX (*21*). The levels of deuterium observed range from 0 to 1 per exchangeable proton, with low levels of incorporation associated with slow H/D exchange rates in the NMR studies (Figure 1D,E). The mass spectrometry results can be classified using analogous H/D exchange rates, with a deuterium incorporation level of ≤0.3 considered slow exchange, a level of ≥0.7 fast exchange, and a level from 0.4 to 0.6 medium exchange. Again, under this classification system, the structured regions in all forms of the protein show slow H/D exchange, while loops and turns generally show fast exchange. For example, the sequence of residues 77−80 (Table 1), which consists of a buried strand of a β-sheet, and residues 99−108 (Table 2), the C-terminal α4 helix, are slow exchanging regions and show low deuterium incorporation levels in all TRXs (Figures 1 and 2). The segment of residues 91−98, on the other hand, is an exposed loop that connects the β5 strand to the α4 helix. The amide hydrogens of the loop exchange relatively rapidly, as is evident from the high levels of deuterium found in both Oxi- and Red-TRX. Similarly, Gly-65, Arg-73, Gly-74, and Ile-75 with fast or medium rates of exchange show moderate to large amounts of deuterium incorporation. Although Thr-89 and Val-91 are present in the central β5 strand, they exhibited greater levels of deuterium, as is consistent with the NMR results. The NMR solution structure indicated that amide protons of these

Table 2: Deuterium Levels Found at Individual Amide Linkages in Fragments of Residues 81−108 (Oxi-, GS-Ethyl-, and Cys-Ethyl-TRX) and 81−101 (Red-TRX) of 20 s Labeled TRXs

	no. of Ds on residue[a]				log k_{ex} (s^{-1})[b]			
residue	Oxi-TRX	Red-TRX	GS-ethyl-TRX	Cys-ethyl-TRX	Oxi-TRX		Red-TRX	
Val-86	0	0	−	−0.2	−2.64	S	−2.57	S
Ala-87	−0.1	0	−0.1	0.3	−4.74	S	−4.75	S
Ala-88	−0.1	−0.1	(0.3)	0	−4.48	S	−4.48	S
Thr-89	0.6	0.4	(0.3)	0.8	−0.6	F	−0.24	F
Lys-90	0	−0.1	(0.8)	0	−3.77	S	−3.69	S
Val-91	0.6	0.4	(0.8)	0.3	*b*	M	*b*	M
Gly-92	0.6	0.5	(0.3)	(0.6)	*b*	M	−0.02	F
Ala-93	0.7	(0.7)	(0.3)	(0.6)	−0.59	F	−0.68	F
Leu-94	0.9	(0.7)	0.9	0.8	−0.48	F	−0.11	F
Ser-95	0.5	0.6	0.7	0.5	*b*	M	*b*	M
Lys-96	0.8	0.7	0.8	0.9	−0.54	F	−0.6	F
Gly-97	(1.0)	(0.8)	0.9	1.0	*b*	M	−0.08	F
Gln-98	(1.0)	(0.8)	(0.5)	1.1	*b*	M	−0.25	F
Leu-99	0.3	0.2	(0.5)	0.1	−3.74	S	−3.84	S
Lys-100	(0.2)	−0.1	0.3	(0)	−5.18	S	−5.14	S
Glu-101	(0.2)	0	0.2	(0)	−5.62	S	−5.54	S
Phe-102	0.1	−	(0.2)	0.1	−4.26	S	−4.28	S
Leu-103	0.2	−	(0.2)	0.1	−7.51	S	−7.47	S
Asp-104	0.2	−	0.1	0	−6.47	S	−6.41	S
Ala-105	0.2	−	0.2	0.1	−3.94	S	−3.8	S
Asn-106	0.1	−	0.3	0.2	−4.21	S	−4.29	S
Leu-107	0.2	−	0.6	0.2	−3.55	S	−3.35	S
Ala-108	0.5	−	1	0.9	*b*	M	*b*	M

[a] In cases of missing fragment ions, the difference of deuterium numbers was equally divided into possible sites as shown in parentheses. [b] The intermediate exchange rates are designated as M, which is in the range of 0.0025−0.25 s^{-1} (log value of −2.6 to −0.6).

Table 3: Deuterium Levels Found at Individual Amide Linkages in Peptide of Residues 28−39 (Oxi-TRX) and 28−37 (Red-, GS-Ethyl-, and Cys-Ethyl-TRX) of 20 s Labeled TRXs[a]

	no. of Ds on residue				log k_{ex} (s^{-1})			
residue	Oxi-TRX	Red-TRX	GS-ethyl-TRX	Cys-ethyl-TRX	Oxi-TRX		Red-TRX	
Trp-31	−	(0.5)	0.5	0.7	−0.55	F	−0.34	F
Cys-32	−	(0.5)	0.9	0.4	0.37	F	*b*	M
Gly-33	−	0.7	(1.0)	1.0	0.14	F	1.16	F
Pro-34								
Cys-35	−	0.7	(1.0)	0.6	−5.07	S	0.4	F
Lys-36	0.6	0.2	0.3	0.3	*b*	M	*b*	M
Met-37	0.3	0.2	0.3	0.4	*b*	M	*b*	M
Ile-38	0.1	−	−	−	−4.28	S	−2.82	S
Ala-39	0.5	−	−	−	−3.08	S	−2.81	S

[a] In cases of missing fragment ions, the difference of deuterium numbers was equally divided into possible sites as shown in parentheses. [b] The intermediate exchange rates are designated as M, which is in the range of 0.0025−0.25 s^{-1} (log value of −2.6 to −0.6).

two residues extend toward the outside of the β-sheet and are not hydrogen-bonded (*14*).

The deuterium levels of the two Cys amino acids at the active site of Oxi-TRX could not be determined by CID MS because the disulfide linkage precludes any cleavage to fragment the two residues at the loop. However, the MS and NMR results for these residues in the Red-TRX form are remarkably similar, with Cys-32 exhibiting medium exchange and Cys-35 fast exchange by both methods. This contrasts with the NMR exchange rates for the active site residues in Oxi-TRX where Cys-32, which sits on a loop, shows fast exchange and Cys-35, which is at one end of a helix, is slow. From the similarity in behavior of the remaining protons within the N-terminal helix, the CID results for the two Cys residues would be expected to mirror the NMR results. The suggestion from both the CID and NMR studies is that Cys-35 becomes less structured upon reduction of the disulfide linkage.

There are some differences in exchange rates seen in the protein by the two methods, but most are relatively minor. For example, Gly-65 which immediately precedes the α3 helix was classified by NMR to be in medium exchange in both Oxi-TRX and Red-TRX but, according to the CID results, changes from medium to fast exchange after reduction. In addition, there are amino acids that the CID method cannot explicitly assign. The individual deuterium contents of Gly-71 and Ile-72 cannot be determined because the peptide linkage between these residues is not cleaved during CID. All deuterium levels listed in parentheses for residues in Tables 1−3 reflect this problem. The interpretation is that the deuteriums are equally shared between the two adjacent amino acids. Overall, however, the CID results and NMR results correlated very well in classifying amide protons along the polypeptide chain according to their respective H/D exchange rates, and in suggesting conformational perturbations resulting from reduction of the disulfide bond at the active site of the protein.

H/D Exchange in GS-Ethyl-TRX and Cys-Ethyl-TRX. The alkyl modifications at Cys-32 of GS-ethyl-TRX and Cys-ethyl-TRX were confirmed by tandem mass spectrometry

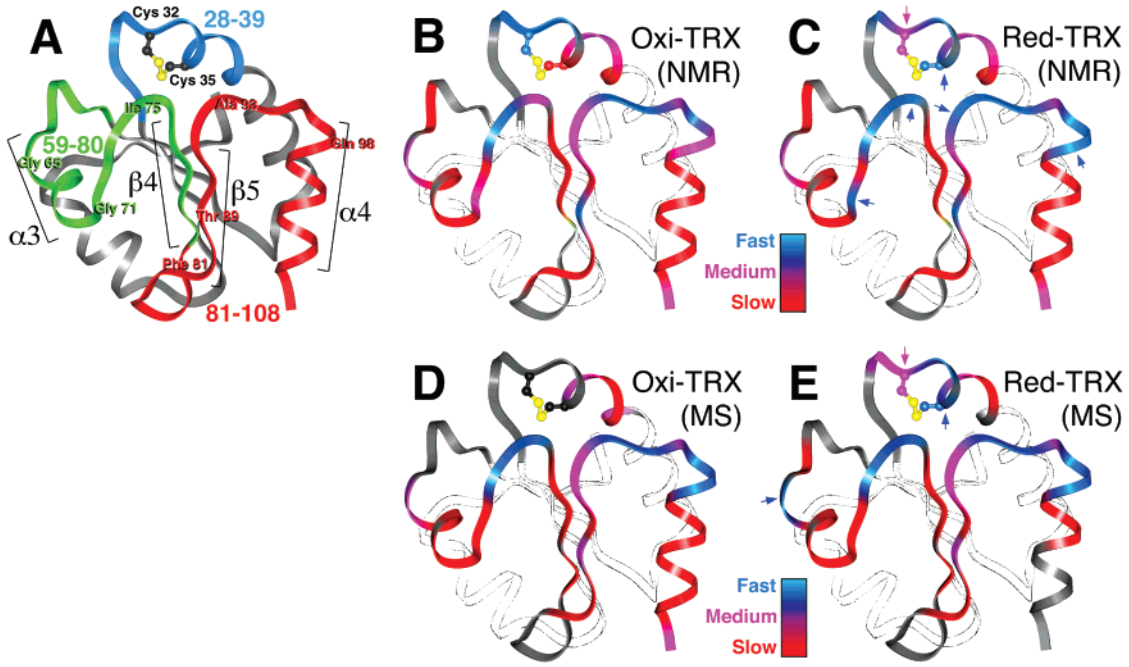

FIGURE 1: H/D exchange of amide protons in thioredoxin in its oxidized (Oxi-TRX) and reduced (Red-TRX) forms. (A) Crystal structure of Oxi-TRX (*22*). The protein is shown as a ribbon diagram tracing the polypeptide backbone. Residues 28−39 (blue), 59−80 (green), and 81−108 (red) represent the peptide fragments used to determine levels of deuterium incorporation by CID MS. The α-helices (α3 and α4) and *β*-strands (*β*4 and *β*5) in these fragments are labeled. This oxidized form of the protein is used for all subsequent figures to provide a common point of reference for comparisons. The cysteine residues in the active site (Cys-32 and Cys-35) are shown with the disulfide linkage of the oxidized protein as ball-and-stick models. Panels B and C compare the rates of H/D exchange determined by NMR (*13*) in the peptide fragments for Oxi-TRX and Red-TRX, respectively. Amide protons with fast exchange rates are in blue, medium rates in purple, and slow rates in red. Changes in the exchange rates upon reduction of the protein are shown with arrows (blue for amides that change to being in fast exchange, purple for medium, and red for slow exchange in Red-TRX). Panels D and E compare the levels of deuterium incorporation seen by CID MS at amide nitrogens of Oxi-TRX and Red-TRX, respectively. Residues that show high levels (≥0.7) of deuterium are considered to be in fast exchange (blue), with low levels of incorporation (≤0.3) in slow exchange (red), and falling between these two levels to be in medium exchange (purple).

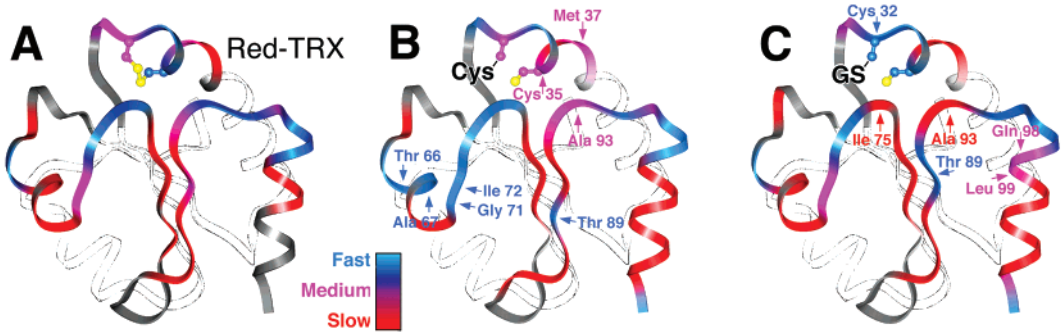

FIGURE 2: Comparison of H/D exchange rates for amide hydrogens in Red-TRX (A), Cys-ethyl-TRX (B), and GS-ethyl-TRX (C). Colors for the polypeptide ribbon are as described in the legend of Figure 1. Arrows indicate amino acids whose exchange rates have changed relative to Red-TRX (blue arrows for those that are in fast exchange, purple in medium exchange, and red in slow exchange in the alkylated proteins compared to Red-TRX). The modifications to Cys-32 are labeled Cys for the ethylcysteinyl chain and GS for the ethylglutathionyl chain.

(*18*). The CID results show that the alkyl chain of the Cys-ethyl-TRX, although small, perturbs the conformation of Red-TRX globally. For the most part, the structured and nonstructured regions are nearly identical in Cys-ethyl-TRX and Red-TRX for all amino acids that can be assigned by this method. The affected amino acids are clustered primarily at the α3 helix, with 3 times as many residues showing faster exchange rates as those that become slower with the ethylcysteinyl modification. For example, the amino acids in the first turn of the α3 helix show the most dramatic increase in the level of deuterieum incorporation, even though they are distant both in sequence and spatially from the modified active site. This localization of amino acids with perturbed rates of H/D exchange away from the active site cysteines suggests that the alkyl Cys chain has an overall destabilizing effect on the stability of the protein's tertiary structure, particularly at the α3 helix.

The amino acids whose H/D exchange rates are most significantly perturbed by the larger ethylglutathionyl group of GS-ethyl-TRX cluster in the vicinity of the modified active site (Figure 2C). Aside from the modified Cys-32, there are twice as many amino acids with reduced H/D exchange rates as those with increased rates when compared to Red-TRX. In particular, Ile-75 and Ala-93 in GS-ethyl-TRX both show

significant reductions in their levels of deuterium incorporation. The H/D exchange rates for the two amino acids are drastically slowed, converting from being rapidly exchanging to being in the slow exchange regime. In addition, the perturbations to the α3 helix and β5 strand in Cys-ethyl-TRX are not seen in GS-ethyl-TRX, suggesting that this larger alkyl modifier has a lesser effect on the overall structure of the protein. Therefore, the H/D exchange rates suggest that the ethylglutathione modification reduces the solvent accessibility around the active site.

The amide protons of the ethylglutathionyl group of GS-ethyl-TRX also appear to be protected from solvent. The CID sees this alkyl modification as a component of residue Cys-32, the amino acid that is modified in the TRX protein. Although the high level of deuterium (0.9) seen at Cys-32 would suggest that this is a highly unstructured residue, it should be stressed that this is distributed to all the amide protons of the ethylglutathionyl chain. If all the protons of the amide nitrogens of this Cys-ethylglutathionyl group were fully exchangeable, a maximum of 3 deuteriums would be expected, counting the 2 exchangeable amide hydrogens of the glutathione and one from Cys-32; therefore, the 0.9 deuterium at this residue is actually low (0.3 deuterium, on average, per amide). The question is the distribution of the isotopes. Because of the absence of cleavage to give the relevant b_n ions between Trp-31 and Cys-32 in Red-TRX, the deuterium level was assigned equally between these two amino acids. In GS-ethyl-TRX and Cys-ethyl-TRX where the CID sequence information is available, Trp-31 has 0.5 and 0.7 deuterium, respectively (Table 3); 0.5 deuterium on Trp-31 of Red-TRX is, therefore, reasonable. On Cys-ethyl-TRX, the deuterium content for the modified Cys-32 is 0.4 or about the same as for Cys-32 of Red-TRX. This is reasonable since the number of Cys-32 amide hydrogens is the same in Red-TRX and Cys-ethyl-TRX. We can estimate, therefore, that 0.4−0.5 deuterium is on the Cys-32 amide of GS-ethyl-TRX, leaving the rest, i.e., ∼0.5, deuteriums on one or both of the amide groups in the ethylglutathionyl chain. Either both these amides are in slow exchange, or one is completely protected; the other shows medium rates of exchange.

DISCUSSION

Molecular Interpretation of H/D Exchange in the Alkyl-Modified TRX Proteins. To interpret the mass spectrometry results for GS-ethyl-TRX at the residue level, we constructed a model for glutathionyl-modified protein independent of the mass spectrometry measurements. No NMR study comparable to those for Oxi-TRX and Red-TRX has been published for the two modified proteins. The most energetically favorable model for GS-ethyl-TRX from molecular simulation places the glutathione chain on a broad surface formed by two loop structures in the protein (Figure 3). These loops include the broad turn (residues 74−77) that connects the α3 helix to the β4 strand, and the loop (residues 90−93) that connects the β5 strand to the α4 helix. The effect of the glutathione modification on the structure of the protein is minimal, with an rmsd of <1.2 Å between the backbone atoms of the modified and unmodified proteins (both after minimization). The most dramatic conformational change is seen in the rotation of the Arg-73 side chain in forming a salt bridge to the γ-Glu of the glutathione chain.

The resulting model (Figure 3B) has the two terminal amino acids of the glutathione chain forming two salt bridges to basic side chains of the protein. The carboxylate group of the γ-Glu residue of the glutathione chain is oriented toward the guanidinium group of residue Arg-73 in the protein, and the carboxy terminus of the glutathione Gly residue toward the amino side chain of Lys-90 in the protein. This results in a net increase in electrostatic stability of −35 kcal for the modified over the unmodified protein.

In addition, the glutathione chain forms three redundant hydrogen bonding interactions with the amide nitrogens and carbonyl oxygens of the protein backbone. The amino termini of the γ-Glu, the γ-oxygen of γ-Glu, and the carbonyl oxygen of the Cys residue of the glutathionyl chain are seen in the model to form hydrogen bonds to the carbonyl oxygen of Arg-73, the amide nitrogen of Ile-75, and the amide nitrogen of Ala-93, respectively, along the peptide backbone of the thioredoxin protein. These hydrogen bonds are estimated to contribute an additional −11.5 kcal of stabilization to the modified protein. Interestingly, the loop that includes Gly-74 and Ile-75 adopts a β-strand conformation in the protein, with ϕ and ψ torsion angles ranging between −140° and 180°. Thus, the interactions with the γ-Glu of the glutathione extension appear to define a mini-β-sheet at the protein surface. From these interactions, the amide nitrogens of both Ile-75 and Ala-93 are predicted to be protected from solvent by the glutathione and, therefore, would show a reduction in their rates of H/D exchange. This is consistent with the H/D exchange data observed in CID studies.

Clearly, the label at Ile-75 of GS-ethyl-TRX is consistent with a hydrogen bond to the γ-carbonyl oxygen of the ethylglutathionyl γ-Glu residue, as predicted from the energy-minimized model. The molecular model of GS-ethyl-TRX also suggests Ala-93 forms a hydrogen bond to the carbonyl oxygen of the glutathionyl cysteine. The experimental results (Table 2) do not allow a distinction between Ala-93 and Gly-92 for the lack of cleavage between these amino acids by CID. However, if 0.5 or 0.6 deuterium is assigned to Gly-92, as is consistent with other TRXs studied here, the deuterium content of Ala-93 would then be ≤0.1, which is consistent with the hydrogen bond predicted by the model. In contrast, the CID results for Cys-ethyl-TRX are consistent with expectations that there are no specific hydrogen bonds from the protein to the alkylcysteinyl chain that would be analogous to that seen with the ethylglutathionyl group. While the salt bridges constrain the ethylglutathionyl moiety to a geometry that allows hydrogen bonding to Ile-75 and Ala-93 in GS-ethyl-TRX, the absence of these interactions should allow the ethylcysteinyl group greater conformational freedom in Cys-ethyl-TRX, thereby reducing the likelihood of any specific hydrogen bonding. Furthermore, on the basis of the H/D exchange already seen, where hydrogen bonding exists, i.e., Ile-75 and Ala-93 in GS-ethyl-TRX, the amount of exchange that takes place at these sites is very low. Hydrogen bonding in structured conformations protects the amide hydrogens against exchange with rate constants that are 10^6-10^8 times smaller than those for random coil-like peptides (*25*), and the amount of labeling at these sites should be very low, if any at all; therefore, we conclude there probably is no hydrogen bonding by the ethylcysteinyl group in Cys-ethyl-TRX.

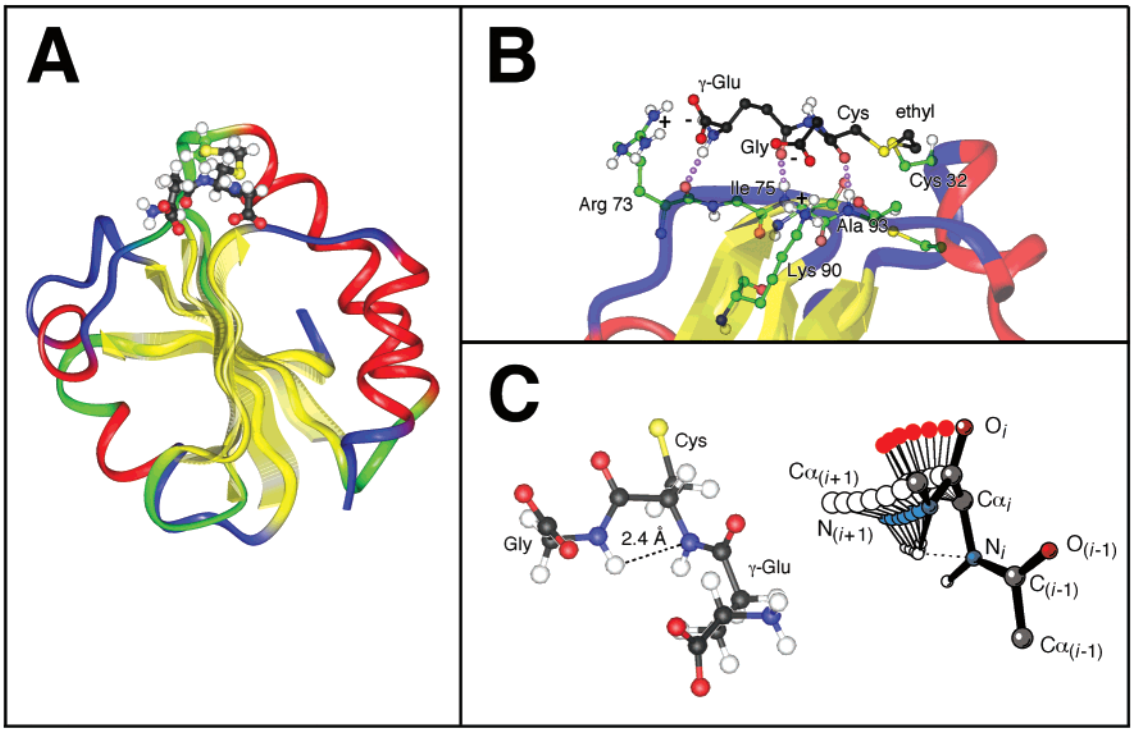

FIGURE 3: Molecular model of GS-ethyl-TRX. (A) Side view of GS-ethyl-TRX. The ethylglutathionyl chain (ball-and-stick model) was attached as an extension from Cys-32 of a reduced thioredoxin model. The red ribbon represents α-helices, and yellow ribbons and arrows represent β-strands; green ribbons are turns, and blue represents unidentified structures as defined in the crystal structure of thioredoxin (*22*). (B) Enlarged view of the ethylglutathionyl interactions with the thioredoxin protein. Carbons of the alkyl chain are shown as black spheres, while those in the thioredoxin protein are shown in green. Oxygen atoms are in red, sulfurs in yellow, and nitrogens in blue. Hydrogen bonding interactions (purple dots) are shown between the glutathione chain and the thioredoxin surface. The positively charged side chains of Arg-73 and Lys-93 are shown to form salt bridges to the negatively charged carboxylate groups of the glutathionyl γ-Glu and Gly residues. (C) The amide−amide hydrogen bond in the molecular model of GS-ethyl-TRX and as seen in single-crystal structures of proteins (*26*). The atoms of the glutathionyl chain (ball-and-stick model) are shown with the hydrogen amide linking the Cys and Gly residues coming within 2.4 Å of the nitrogen of the amide linking the Cys to the γ-Glu residue. For comparison, the various geometries of dipeptides, with various values for the ϕ torsion angle seen in high-resolution protein structures, are shown that place amide hydrogens in the proximity of the nitrogen of an adjacent amide (*26*).

The deuterium observed to be incorporated at the Cys-32 residue of GS-ethyl-TRX includes the exchangeable amide hydrogens at this amino acid as well as the Cys and Gly residues of the glutathione chain, since the method does not distinguish the GS-ethyl modification from the modified amino acid of TRX. If we assume that the residue in GS-ethyl-TRX behaves in a fashion similar to that in the Cys-ethyl-TRX protein, the Cys-32 from the protein would account for 0.4 of the 0.9 deuterium that is observed. This leaves 0.5 deuterium for the two amides of the glutathione chain. If these are equally distributed between the glutathione Cys and Gly residues, the amide hydrogens of the GS-ethyl chain would be considered to be in slow exchange. However, the molecular model suggests that both these amides sit on the solvent-exposed surface of the molecule and, therefore, should be in moderate to fast exchange. One possible resolution to this problem would be that the glutathione chain has the two peptide bonds oriented toward the protein, rather than exposed to solvent, as is seen in the molecular model. However, such a model would not allow the corresponding carbonyl groups of the glutathione to form hydrogen bonds to, and thereby protect the amide protons of, Ile-75 and Ala-93 of the protein, as was observed in the CID results. An alternative suggestion is that one of the amide nitrogens is involved in a hydrogen bonding interaction and, therefore, becomes protected from solvent exchange. For example, the amide hydrogen of the glutathionyl Gly residue could form a hydrogen bond either to the carbonyl oxygen of the γ-Glu or to the Cys amide nitrogen. The molecular model suggests the latter to be more likely.

The geometry of the amino groups at the glutathionyl Gly and Cys residues in the model is very similar to that described by Karplus (*26*) in which the N−H group of one peptide bond is oriented perpendicular to the plane of the adjacent peptide (Figure 3C). Such an arrangement would allow a hydrogen bond to form with the amide hydrogen of one peptide serving as the donor and the π-electrons of the second peptide plane as the acceptor. Although unusual, a number of single-crystal structures of proteins place peptides in this geometry and in this region of the ϕ and ψ torsion angle (Ramachandran) plots that would normally be considered disallowed. In the current model, the amide H of the Gly is placed ∼2.4 Å from the N atom of the Cys, and ϕ and ψ torsional angles around the Cα carbon are −108° and −14°, respectively. These parameters are within the ranges defined previously for this type of amide to amide hydrogen bonding interaction (*26*). Thus, this type of amide to amide hydrogen bonding interaction is not unprecedented.

While a second hydrogen bond to the γ-Glu carbonyl oxygen cannot be ruled out, the torsional strain may preclude this type of interaction. Forcing the amino nitrogen to form a hydrogen bond to any other group will necessarily disrupt

the hydrogen bonds that have been defined independently by the mass spectrometry H/D results and molecular simulation. For example, for this amino group to form a second hydrogen bond to the carbonyl oxygen of the γ-Glu, which is ~4.5 Å away, would require a torsional rotation of either ψ by 60° or ϕ by 60°. In both cases, the hydrogen bonds to the amino groups of Ile-75 and Ala-93 would be lost, which would directly contradict the H/D exchange results. With these interactions, only one extra amide hydrogen remains available for exchange and the extra 0.5 deuterium on the ethylglutathionyl group of GS-ethyl-TRX can reasonably be assigned to the Cys amide.

CONCLUSIONS

These studies have shown that amide site specific hydrogen bonding interactions can be detected by H/D exchange and electrospray ionization mass spectrometry. Site specific hydrogen isotope exchange/mass spectrometric protocols complement NMR methods which have been the standard and most reliable approaches available for examining protein structural effects in solution for almost 30 years. In addition, the differences in H/D exchange seen in the GS-ethyl-TRX and Cys-ethyl-TRX proteins can be rationalized at the molecular level. In the case of GS-ethyl-TRX, they corroborate the hydrogen bonding patterns predicted from a molecular structure derived from molecular simulation.

There are structural similarities between TTase-SSG and GS-ethyl-TRX. They each have four or five central parallel and antiparallel β-sheets surrounded by multiple α-helices that form a cleft that is spanned by the extended glutathionyl or ethylglutathionyl group, respectively. There are further similarities in the hydrogen bonding patterns between these two modified proteins. From simulated structures and NMR NOE data, salt bridges were inferred between guanidinium groups of arginines in the protein and the carboxylate groups of γ-Glu and Gly of the glutathionyl moiety in TTase-SSG (*17*). Hydrogen bonding interactions identified between the valine amide H in the protein and the carbonyl oxygen of the γ-Glu and the cysteinyl carbonyl oxygen of the glutathionyl group stabilize the structure further. Hydrogen bonding interactions in some loop and turn regions, as seen in Ala-93 and Ile-75 of GS-ethyl-TRX, were also detected in TTase-SSG.

While the ethylglutathionyl group in GS-ethyl-TRX and the glutathionyl group in TTase-SSG form salt bridges and other hydrogen bonding interactions, the smaller cysteinyl group in Cys-ethyl-TRX apparently cannot do so. Interestingly, however, the cysteinyl group may disrupt certain hydrogen bonds as suggested by the high levels of deuterium located on Thr-66, Ala-67, and Ile-72 in the α3 helix. Similarly, hydrogen bonding interactions in Asn-63 and Ile-72 in the α3 helix and Lys-90 in the β5 sheet may also be disrupted in GS-ethyl-TRX as suggested by the high levels of deuterium at these residues.

There are clear advantages and disadvantages with both NMR and mass spectrometry as methods for monitoring H/D exchange, particularly in studying protein conformations. The advantages in using mass spectrometry are related to the sensitivity, size, and purity of the proteins. The much greater sensitivity of mass spectrometry not only allows studies with minimal amounts of protein but also circumvents the problems with aggregation that can occur at high sample concentrations. In terms of the analysis, the size of the protein that can be studied depends mostly on the size of the peptic peptides that can be produced and separated by liquid chromatography in the LC−MS system. And when LC−MS is used, the purity of the sample also is not quite so critical. The disadvantages of mass spectrometry are related to incomplete sequence information and the potential inaccuracies associated with label scrambling during CID. The "mobile proton" model (*27*) wherein a proton migrates from a protonated amino side chain of the peptide to an amide nitrogen (Scheme 1) may suggest that reliable H/D data by CID MS/MS would be difficult to obtain. The key to measuring accurate H/D ratios, however, may lie in the mechanism postulated by Harrison and co-workers (*28*) in which fragmentation occurs by displacement of the protonated amide site via formation of a protonated oxazolone structure as a b_n ion (Scheme 2). The amide site to which the proton was originally transferred becomes the leaving group and is, therefore, of no further consequence in the analysis. There could, of course, be other factors that determine the success or failure of these types of measurements, not the least of which is the protein being analyzed. Fortunately, studies from our group (*21*) and others (*29*) show that quite reliable information can be obtained in at least some cases on the deuterium content of peptide amide sites when b_n ions are used for the analyses.

Scheme 1

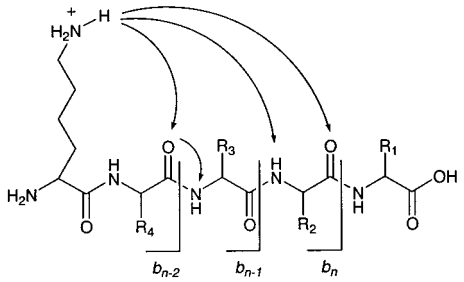

Scheme 2

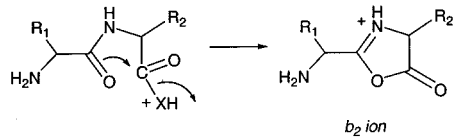

REFERENCES

1. Radford, S. E., Woolfwon, D. N., Martin, S. R., Lowe, G., and Dobson, C. M. (1991) *Biochem. J. 273*, 211−217.
2. Eyles, S. J., Radford, S. E., Robinson, C. V., and Dobson, C. M. (1994) *Biochemistry 33*, 13038−13048.
3. Resing, K. A., and Ahn, N. G. (1998) *Biochemistry 37*, 463−475.
4. Miranker, A., Robinson, C. V., Radford, S. E., Aplin, R. T., and Dobson, C. M. (1993) *Science 262*, 896−900.
5. Bai, Y., Sosnick, T. R., Mayne, L., and Englander, S. W. (1995) *Science 269*, 192−197.
6. Yang, H., and Smith, D. L. (1997) *Biochemistry 36*, 14992−14999.
7. Chung, E. W., Nettleton, E. J., Morgan, C. J., Gross, M., Miranker, A., Radford, S. E., Dobson, C. M., and Robinson, C. V. (1997) *Protein Sci. 6*, 1316−1324.
8. Eyles, S. J., Dresch, T., Gierasch, L. M., and Kaltashov, I. A. (1999) *J. Mass Spectrom. 34*, 1289−1295.

9. Arrington, C. B., Teesch, L. M., and Robertson, A. D. (1999) *J. Mol. Biol. 285*, 1265−1275.
10. Maier, C. S., Schimerlik, M. I., and Deinzer, M. L. (1999) *Biochemistry 38*, 1136−1143.
11. Katti, S. K., LeMaster, D. M., and Eklund, H. (1990) *J. Mol. Biol. 212*, 167−184.
12. Dyson, H. J., Gippert, G. P., Case, D. A., Holmgren, A., and Wright, P. E. (1990) *Biochemistry 29*, 4129−4136.
13. Jeng, M.-F., and Dyson, H. J. (1995) *Biochemistry 34*, 611−619.
14. Jeng, M.-F., Campbell, A. P., Begley, T., Holmgren, A., Case, D. A., Wright, P. E., and Dyson, H. J. (1994) *Structure 2*, 853−868.
15. Holmgren, A., and Björnstedt, M. (1995) *Methods Enzymol. 252*, 199−208.
16. Jeng, M.-F., Reymond, M. T., Tennant, L. L., Holmgren, A., and Dyson, H. J. (1998) *Eur. J. Biochem. 257*, 299−308.
17. Yang, Y., Jao, S.-C., Nanduri, S., Starke, D. W., Mieyal, J. J., and Qin, J. (1998) *Biochemistry 37*, 17145−17156.
18. Erve, J. C. L., Barofsky, E., Barofsky, D. F., Deinzer, M. L., and Reed, D. J. (1995) *Chem. Res. Toxicol. 8*, 934−941.
19. Humphreys, W. G., Kim, D.-H., Cmarik, J. L., Shimada, T., and Guengerich, F. P. (1990) *Biochemistry 29*, 10342−10350.
20. Ozawa, N., and Guengerich, F. P. (1983) *Proc. Natl. Acad. Sci. U.S.A. 80*, 5266−5270.
21. Kim, M.-Y., Maier, C. S., Reed, D. J., and Deinzer, M. L. (2001) *J. Am. Chem. Soc. 123*, 9860−9866.
22. Schultz, L. W., Chivers, P. T., and Raines, R. T. (1999) *Acta Crystallogr. D55*, 1533−1538.
23. Cornell, W. D., Cieplak, P., Bayly, C. I., Gould, I. R., Merz, K. M., Jr., Ferguson, D. M., Spellmeyer, D. C., Fox, T., Caldwell, J. W., and Kollman, P. A. (1995) *J. Am. Chem. Soc. 117*, 5179−5197.
24. Wang, J., Cieplak, P., and Kollman, P. A. (2000) *J. Comput. Chem. 21*, 1049−1074.
25. Bai, Y., Milne, J. S., Mayne, L., and Englander, S. W. (1994) *Proteins 20*, 4−14.
26. Karplus, P. A. (1996) *Protein Sci. 5*, 1406−1420.
27. Dongré, A. R., Jones, J. L., Somogyi, A., and Wysocki, V. H. (1996) *J. Am. Chem. Soc. 118*, 8365−8374.
28. Harrison, A. G., Csizmadia, I. G., and Tang, T.-H. (2000) *J. Am. Soc. Mass Spectrom. 11*, 427−436.
29. Deng, Y., Pan, H., and Smith, D. L. (1999) *J. Am. Chem. Soc. 121*, 1966−1967.

BI0115941